

Article

Validation of a Multi-Segment Kinematic Foot Model and Optical Motion Capture Using Bi-Planar X-Ray Fluoroscopy and a Markerless RSA Approach

Aida Valevicius ¹, Kristen Bushey ² and Thomas Jenkyn ^{1,2,*}¹ Department of Mechanical and Materials Engineering, Faculty of Engineering, University of Western Ontario, London, ON N6A 3K7, Canada² Fowler Kennedy Sport Medicine Clinic, University of Western Ontario, London, ON N6A 3K7, Canada

* Correspondence: tjenkyn@uwo.ca

Abstract: Gait analysis with optical motion capture typically treats the foot as a single segment, which can measure clinically useful kinematics but is insufficient to measure the kinematics of joint motions within the foot. This study hypothesizes that a four-segment foot model, tracking the hindfoot, midfoot, forefoot, and hallux, can accurately measure intrinsic foot kinematics when validated against the gold standard of fluoroscopic X-ray radiostereometric analysis (RSA) during walking gait. Ten healthy volunteers were tested, with the left foot tracked during the stance phase from heel strike to toe off. The results indicated that the height-to-length ratio of the medial longitudinal arch (MLA) and the transverse plane motion of the hindfoot were the most reliable kinematic measures, showing the best agreement between the optical motion capture and RSA methods. In contrast, the frontal plane motions of the hindfoot and forefoot showed the greatest differences, though these were not statistically significant at $p < 0.05$. These findings demonstrate that the multi-segment foot model is a valid method for measuring intrinsic foot kinematics in a clinical setting, providing a reliable alternative to more invasive techniques.



Citation: Valevicius, A.; Bushey, K.; Jenkyn, T. Validation of a Multi-Segment Kinematic Foot Model and Optical Motion Capture Using Bi-Planar X-Ray Fluoroscopy and a Markerless RSA Approach. *Appl. Sci.* **2024**, *14*, 11285. <https://doi.org/10.3390/app142311285>

Academic Editor: Arkady Voloshin

Received: 29 September 2023

Revised: 12 September 2024

Accepted: 28 October 2024

Published: 3 December 2024



Copyright: © 2024 by the authors. Licensee MDPI, Basel, Switzerland. This article is an open access article distributed under the terms and conditions of the Creative Commons Attribution (CC BY) license (<https://creativecommons.org/licenses/by/4.0/>).

Keywords: gait; foot kinematics; multi-segment model; biomechanics; radiostereometric analysis; fluoroscopy

1. Introduction

Clinical gait analysis using optical motion capture typically assumes the foot to be a single rigid segment. This approach is useful since it is simple and can easily measure clinically useful kinematics such as the progression angle of the foot, the dorsi/plantar flexion of the ankle joint, and the inversion/eversion of the subtalar joint [1–3]. However, this approach is insufficient when kinematic information is needed about the motions of the joints within the foot, such as between the hindfoot and midfoot or the midfoot and the forefoot, since these motions cannot be measured when the foot is assumed to be a single rigid segment.

The joints of the foot work together with the ankle and subtalar joints during gait, allowing for flexibility of the foot and the safe transfer of large biomechanical loads during walking [4–6]. At the beginning of the stance phase during walking gait, the foot is a flexible and compliant structure, allowing it to safely land on the walking surface and absorb inertial loading from the decelerating body. Later in the stance phase, the foot transitions into a rigid structure through which large propulsive forces can be applied to the ground. This dual function of the foot is often disrupted by injury and pathology. Therefore, measuring the motion of the joints of the foot during functional, weight-bearing activities such as walking is clinically necessary [1–4,7–10].

Measuring foot joint motion requires that several segments within the foot be tracked. Several multi-segment foot models have been described in the literature. But there is not yet consensus on how the segments of the foot should be defined. The multi-segment foot

model used in this study was developed by Jenkyn and Anas [11]. This model tracks the foot as four connected segments: the hindfoot (calcaneus), midfoot (three cuneiforms, navicular, and cuboid), forefoot (metatarsals), and hallux [11].

Optical motion capture tracks reflective markers attached at various anatomical landmarks on the body. Three markers per rigid segment can track the six-degree-of-freedom pose of the segment [7–9]. While optical motion capture has the advantage of allowing the patient great freedom of movement, its limitation is that the reflective markers must be attached to the skin or clothing. Therefore, there is always an amount of relative motion between the markers and the underlying bones [12]. Multi-segment foot models require more reflective markers to be attached to the foot than the usual three. How much more kinematic error arises due to these extra markers is unknown, and the effect on the inter-segmental measurements within the foot is unknown. This limits the clinical adoption of multi-segment foot models [4–10].

A more accurate method for tracking bone kinematics is available with bi-planar fluoroscopic radiostereometric analysis (RSA) [12–15]. X-ray fluoroscopy allows for the direct and simultaneous visualization of the skin-mounted markers of the optical system and the bones themselves during dynamic, weight-bearing activity. Bi-planar fluoroscopy images the bones of interest from two different angles. The RSA method determines the six-degree-of-freedom pose of each bone with respect to time [12–16]. The accuracy of fluoroscopic RSA has been demonstrated to be superior to optical motion capture in the foot [14,15].

In the current study, the kinematics of the joints of the foot are measured using the multi-segment foot model with optical motion capture and bi-planar fluoroscopic RSA simultaneously. The purpose of this study is to validate the intersegment kinematics as measured with the multi-segment foot model and quantify the errors arising from relative motion between the reflective markers and the underlying bones. This is performed in healthy volunteers during a fully weight-bearing walking gait.

2. Materials and Methods

2.1. Test Volunteers

Ten healthy young adults (7 males, 3 females; 26 ± 5.7 years; height 175 ± 10.6 cm; weight 71.8 ± 14.8 kg; foot length 25.1 ± 2.6 cm) were recruited for this study. None of the participants had prior or on-going foot injury or pathology. The institution's Research Ethics Board for Health Science approved this study, and all participants gave their informed, signed consent.

2.2. Optical Data Collection and Multi-Segment Foot Model

A six-camera optical motion capture system (2 Eagle/4 Hawk HiRes cameras, Cortex 2.6 system, Motion Analysis Corp., Santa Rosa, CA, USA) was used to capture the kinematics of left and right legs and feet. Ten auto-reflective spherical markers of 1 cm diameter were placed on the left and right knees on the fibular head, left and right lower legs midcalf, left and right heels, the left and right lateral and medial malleoli, and on the dorsum of the right foot at the head of the second metatarsal (Figure 1). These markers track the motion of the lower leg segments. On the left foot, five 3-marker clusters were placed to track the four segments of the multi-segment foot model (Figure 1), as per Jenkyn and Anas [3]. All testing was performed barefoot. The segments of the left foot were tracked with five 3-marker clusters on the lateral posterior calcaneus (hindfoot), dorsal medial navicular (midfoot), midshaft first and fifth metatarsals (forefoot), and the dorsum of the first phalanx of the great toe (hallux). Kinematic data were sampled at 60 frames per second. Kinematic data were low-pass filtered with a 4th-order Butterworth smoothing zero-lag filter with a cut-off frequency of 6 Hz. This was performed to remove vibration artefacts from the marker clusters.



Figure 1. Placement of the auto-reflective markers on the lower legs and feet. Testing was performed barefoot. The lower legs and right foot were tracked with individual spherical markers (**left**). The segments of the left foot were tracked with five 3-marker clusters on the lateral posterior calcaneus (hindfoot), dorsal medial navicular (midfoot), midshaft first and fifth metatarsals (forefoot), and the dorsum of the first phalanx of the great toe (hallux). This is shown in close-up in the photograph to the (**right**).

2.3. Fluoroscopy RSA Data Collection

Two X-ray fluoroscopes (SIREMOBIL Compact (L); Siemens Medical Solutions USA Inc., Malvern, PA, USA) were positioned to provide two views of the planted left foot from different angles (Figure 2). One view was a sagittal, lateral view, and the other an oblique anterior/posterior view of the foot [15]. A raised wooden platform allowed each participant to walk through the view volume of the two fluoroscopes. In each trial, the left foot was planted in the view volume (Figure 2) as the participant walked at their preferred speed of walking. Participants wore a leaded thyroid shield, wrap-around vest and kilt for protection from X-ray exposure. Fluoroscopic images were collected synchronously at 30 frames per second. In each fluoroscopic image, both the bones of the left foot and the marker clusters of the multi-segment foot model are visualized.

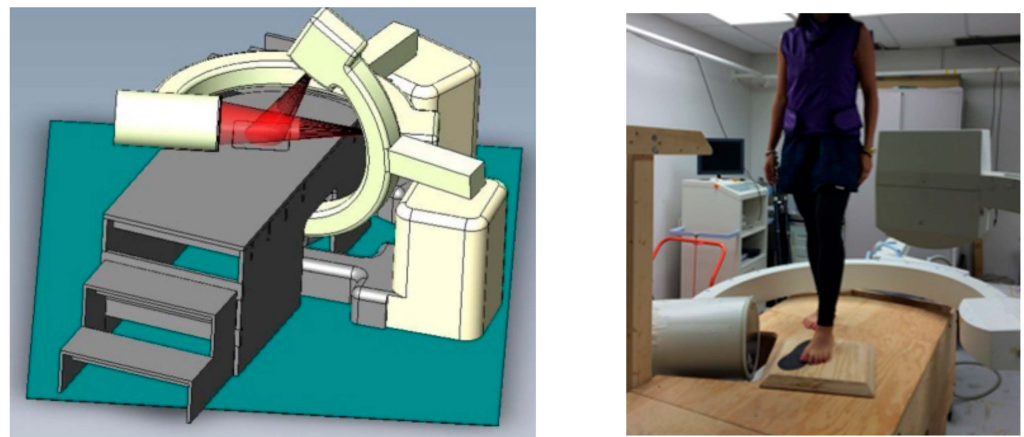


Figure 2. Diagram of the positioning of the two X-ray fluoroscopes with respect to the raised wooden platform (**left**). Each participant walked at their preferred speed of walking, planting the left foot in the view volume of the two fluoroscopes (**right**). Testing was performed barefoot.

2.4. Testing Protocol

Participants underwent optical motion capture and bi-planar fluoroscopic RSA simultaneously. First, each subject stood quietly with the left foot in the view volume and the right foot slightly behind and at shoulder width apart. This established the static, weight-bearing position for each intersegmental foot joint and the MLA. After having time to familiarize themselves with walking on the raised walkway, each participant performed four walking trials. If the left foot was misplaced within the view volume or the fluoroscopic image quality was of poor quality, the trial was repeated.

2.5. Data Analysis

Prior to the testing session, each study participant had a CT taken of their left foot. From the CT, surface models were created of each foot bone of interest for tracking with the fluoroscopic images [15]. The five segments of the foot as defined by the multi-segment foot model are tracked via both systems. The calcaneus bone is compared to the hindfoot segment. The tarsal bones, navicular, cuboid, and three cuneiforms are compared to the midfoot segment. The first metatarsal is compared to the medial forefoot segment. The fifth metatarsal is compared to the lateral forefoot segment, and the proximal phalanx of the great toe is compared to the hallux segment of the multi-segment foot model. Joint angles between each segment were calculated using the method of Valevicius, 2014 [16]. The height-to-length ratio of the medial longitudinal arch (MLA) is recreated from the fluoroscopy RSA data as the ratio of the right-angle distance of the navicular tuberosity (NT) to the vector connecting the medial posterior border of the calcaneus (MP) and the head of the first metatarsal (MH) in the sagittal plane as shown in Figure 3.

To ensure the optical motion capture and fluoroscopic data were synchronized, the instant of left foot strike in both data sets was aligned. In the optical motion capture data set, this was defined as when the displacement of the heel marker cluster in the vertical direction reached its minimum after descending toward the platform surface. In the fluoroscopy RSA data set, this was defined as when the calcaneus bone displacement reached its minimum in the vertical direction. These frames of data were aligned as the start of the stance phase for the left foot. Similarly, the instant of toe off was aligned. This was defined by the hallux marker cluster beginning to displace upwards showing that the first phalanx of the great toe is displacing upwards. These frames were aligned as the end of stance phase for the left foot. Once the data sets were aligned, the discrete data points in each set were interpolated into 101 data points from 0% to 100% of the stance phase.

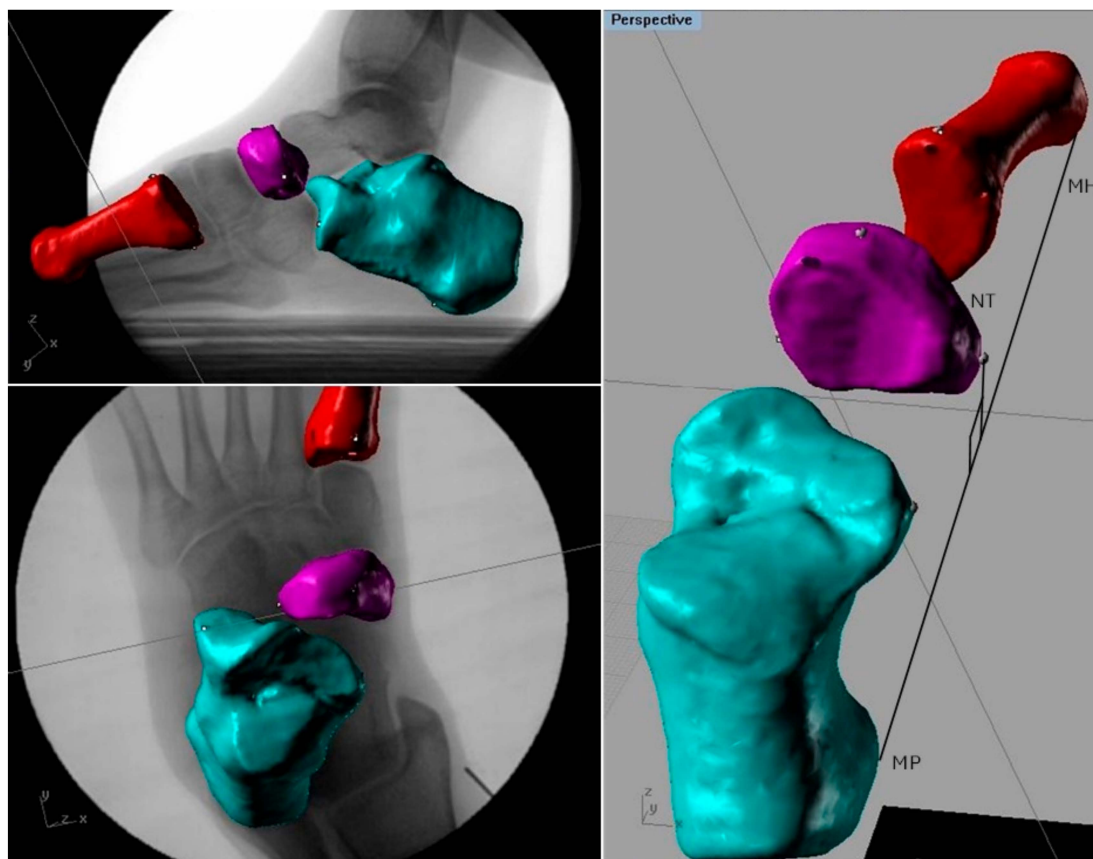


Figure 3. The calcaneus (blue bone), navicular (purple bone) and first metatarsal (red bone) were each tracked individually. The height-to-length ratio of the medial longitudinal arch was calculated as the ratio of the right-angle distance of the navicular tuberosity (NT) to the vector connecting the medial posterior border of the calcaneus (MP) and the head of the first metatarsal (MH) in the sagittal plane, as shown.

2.6. Statistic Analysis

The first, middle, and last 5% of each optical motion capture trial was averaged and used as a comparison to the first, middle, and last stance phase value from the fluoroscopic RSA data. These values were averaged for each joint motion and an independent samples *t*-test was run using SPSS v25 (IBM Corporation, Armonk, NY, USA) on the heel strike, midstance, and toe off values between motion capture and fluoroscopic data to test for statistical difference. Statistical significance was set at $p = 0.05$. The power was set with an alpha of 0.05 and a beta of 0.80. With the greatest standard deviation of 2.54° seen for forefoot supination/pronation and 0.005 for the MLA height-to-length ratio, effect sizes of 3.5° and ratios of 0.007 required 8.2 test subjects. Therefore, 10 test subjects were conservative.

3. Results

Table 1 shows the comparison of the range of intersegmental joint angular motion during the stance phase and the maximum and minimum values for each range measured using optical motion capture and fluoroscopic RSA. The motions reported are for hindfoot supination/pronation, hindfoot internal/external rotation, forefoot supination/pronation, and the height-to-length ratio of the MLA. These are reported in degrees, except for the MLA height-to-length ratio, and averaged over all subjects. The values for the MLA height-to-length ratio values have been normalized to quiet standing, which is 0. Positive means a higher arch, negative means a lower arch.

Table 1. Comparison between optical motion capture and fluoroscopic RSA measurements of intersegmental joint motions over all trials for all subjects. The range, maximum, and minimum values are given in degrees except for the MLA, which is reported as the ratio normalized to 0 in quiet standing.

Joint Motion (°)	Range		Maximum–Minimum	
	Motion Capture	Fluoroscopy	Motion Capture	Fluoroscopy
Hindfoot				
Supination/pronation (°)	15.80	8.05	(2.43, −13.37)	(3.86, −4.19)
Internal/external rotation (°)	13.16	8.70	(5.93, −7.23)	(4.57, −4.13)
Forefoot	18.27	10.18	(14.51, −3.76)	(12.07, 1.89)
MLA height-to-length ratio	0.12	0.02	(0.09, −0.03)	(0.00, −0.02)

The greatest difference in angular motion between the two datasets was for forefoot supination/pronation. The range of forefoot segment motion in the frontal plane with respect to the midfoot was 18.27° and 10.18° for optical motion capture and fluoroscopy, respectively. Overall, the optical motion capture values for the range of intersegmental joint motion tended to overestimate the motion when compared to fluoroscopic RSA.

Table 2 compares the average angle value for heel strike, midstance, and toe off measured with optical motion capture and fluoroscopic RSA as an average of all trials for each foot joint motion examined. Angle values during mid-stance were the most similar when comparing motion capture and fluoroscopy. An asterisk indicates there is a significant difference between optical motion capture and fluoroscopic RSA values. The level of significance was set to $p < 0.05$. From this table, the only significant difference between motion capture and fluoroscopy was found at the level of the MLA height-to-length ratio for mid-stance and toe off.

Table 2. Comparison of average angle values and normalized MLA height-to-length ratio for heel strike, midstance, and toe off measured with optical motion capture and fluoroscopic RSA. The asterisk indicates a significant difference of $p < 0.05$.

Joint Motion (°)	Heel Strike		Midstance		Toe Off	
	Motion Capture	Fluoroscopy	Motion Capture	Fluoroscopy	Motion Capture	Fluoroscopy
Hindfoot						
Supination/pronation (°)	−8.10	−3.66	−4.37	0.75	−3.06	3.65
Internal/external rotation (°)	2.48	3.82	−0.23	−0.67	−4.53	−3.58
Forefoot	19.41	11.73	1.45	3.26	−10.78	2.85
MLA height-to-length ratio	−0.01	−0.01	0.02 *	0.00 *	0.05 *	0.00 *

Table 3 displays the difference in angles between optical motion capture and fluoroscopic RSA for all foot joint motions. For supination/pronation of the hindfoot, the smallest difference between both motion capture techniques was seen at heel strike. For internal/external rotation of the hindfoot, the smallest difference was seen at midstance. For forefoot motion, the smallest difference was also seen at midstance. For the MLA height-to-length ratio at heel strike, there was no difference seen between the value obtained from motion capture and fluoroscopy. There is no consistent trend in the joint angles of the optical motion capture over-estimating or under-estimating fluoroscopic RSA. The largest limits of agreement were for the supination/pronation of the forefoot, with values of 3.6 to 11.8°, suggesting that 95% of the differences between the two methods fall within this range. The standard deviation of the differences for forefoot supination/pronation was smaller than the standard deviation for the study population. There was no evidence of a proportional bias, and the difference between the two measurement methods did not increase with the magnitude of the angles.

The average amount of hindfoot supination/pronation (Figure 4), hindfoot internal/external rotation (Figure 5), forefoot supination/pronation (Figure 6), and the normalized MLA height-to-length ratio (Figure 7) are all shown at heel strike, midstance, and toe off for optical motion capture and fluoroscopic RSA. In each figure, error bars indicate one standard error above and below the mean. A significant difference of $p < 0.05$ between the two measurement methods is indicated by an asterisk.

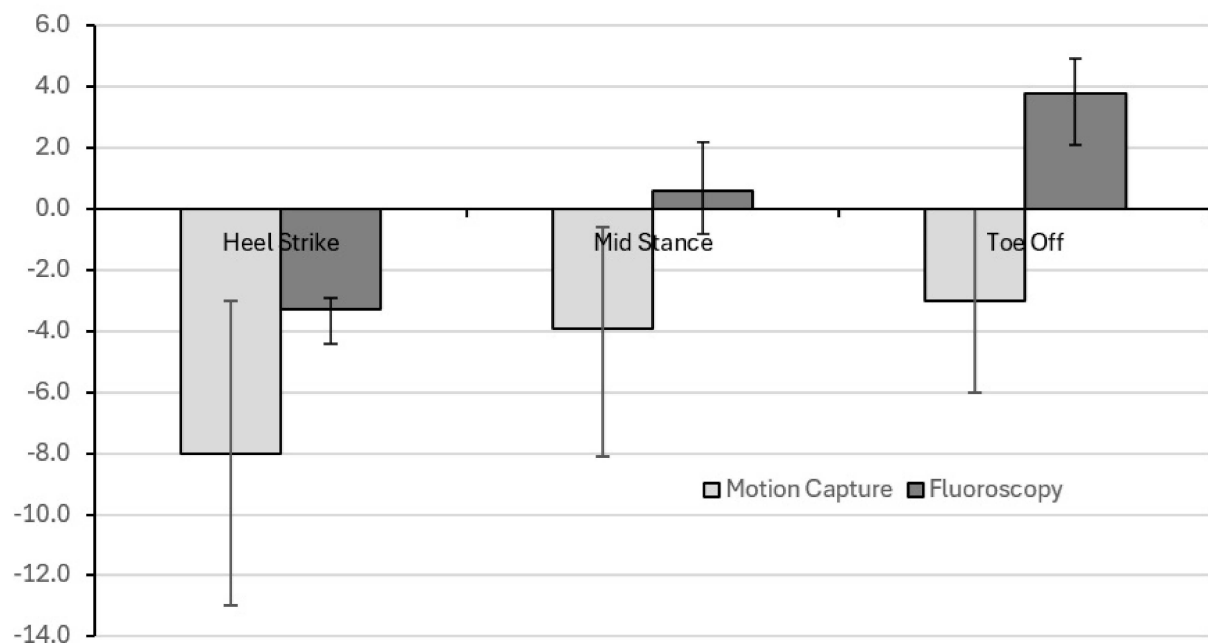


Figure 4. Average hindfoot supination/pronation at heel strike, midstance, and toe off for optical motion capture and fluoroscopic RSA. A positive angle means more supination than quiet standing. Error bars indicate one standard error above and below the mean.

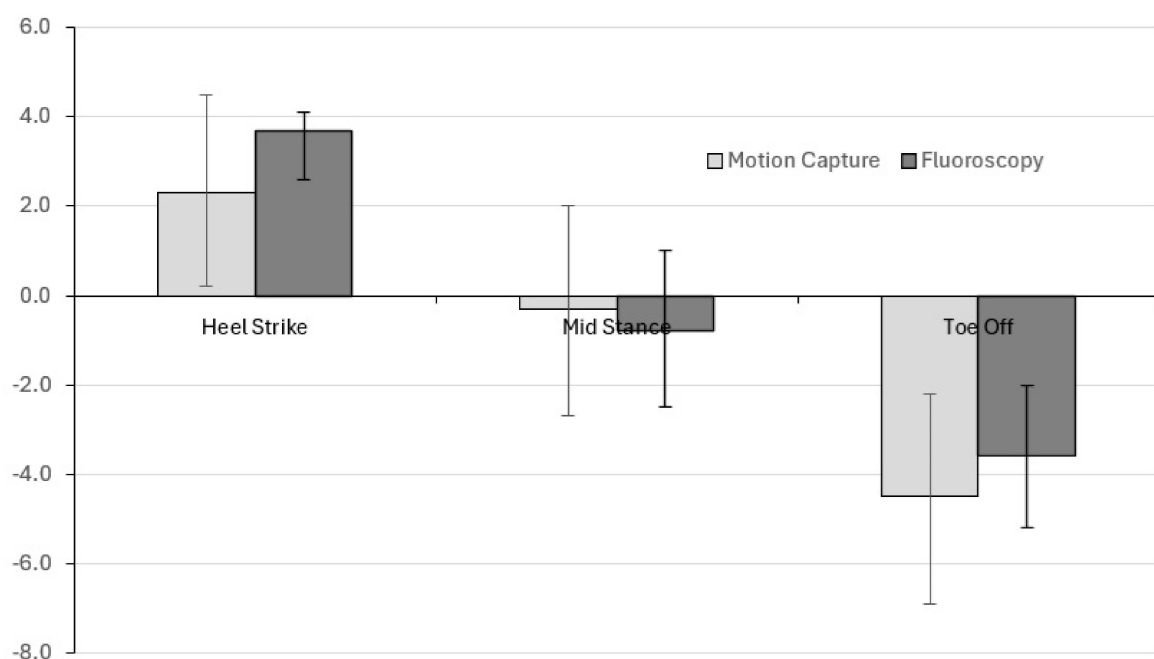


Figure 5. Average hindfoot internal/external rotation at heel strike, midstance, and toe off for optical motion capture and fluoroscopic RSA. A positive angle means more internal rotation than quiet standing. Error bars indicate one standard error above and below the mean.

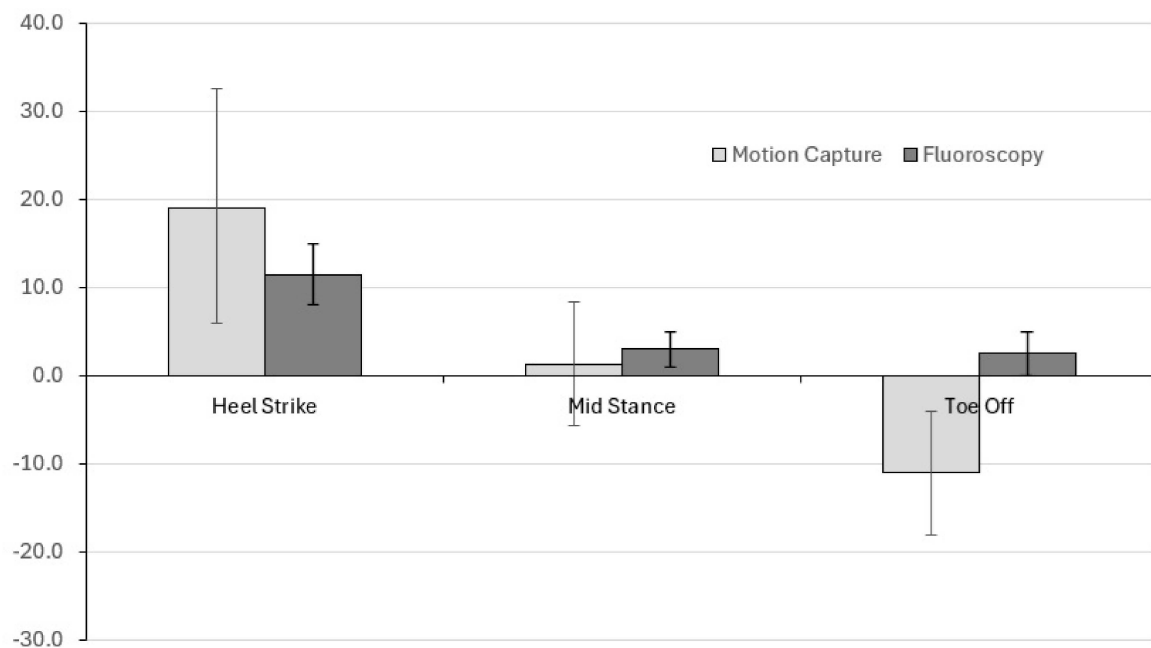


Figure 6. Average forefoot supination/pronation at heel strike, midstance, and toe off for optical motion capture and fluoroscopic RSA. A positive angle means more supination than quiet standing. Error bars indicate one standard error above and below the mean.

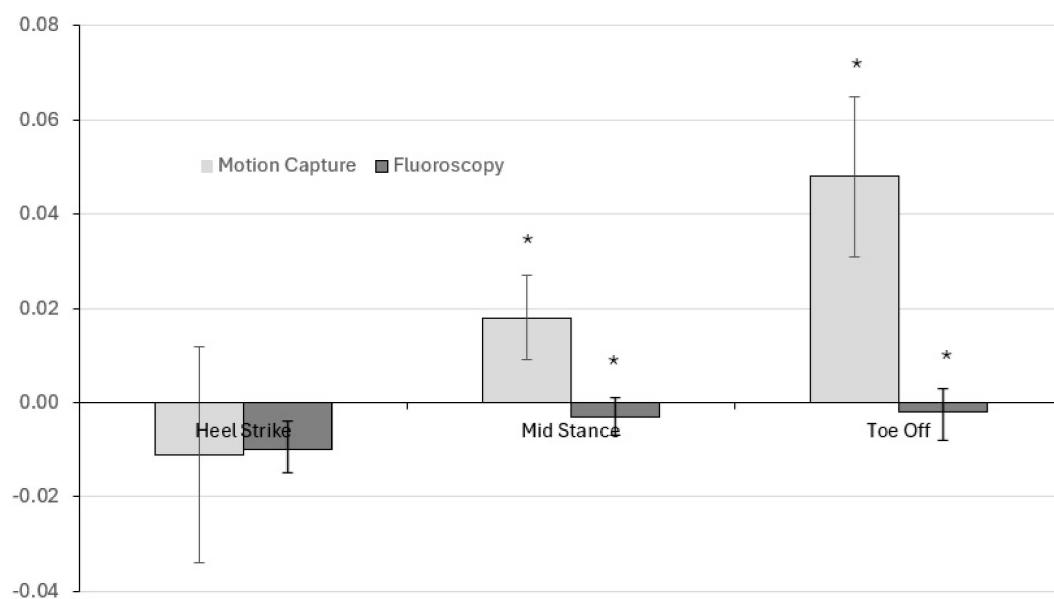


Figure 7. Average normalized MLA height-to-length ratio at heel strike, midstance, and toe off for optical motion capture and fluoroscopic RSA. A positive ratio means the arch is higher than at quiet standing. Negative means the arch is lower. Error bars indicate one standard error above and below the mean. A significant difference of $p < 0.05$ between the two measurement methods is indicated by an asterisk.

Table 3. Difference in the angles between optical motion capture and fluoroscopic RSA for all foot joint motions and the normalized MLA height-to-length ratio.

	Heel Strike	Midstance	Toe Off
Hindfoot			
Supination/pronation (°)	−4.45	−5.12	−6.70
Internal/external rotation (°)	−1.33	0.45	−0.95
Forefoot (°)	7.68	−1.81	−13.63
MLA height-to-length ratio	0.00	0.02	0.05

4. Discussion

Quantifying errors in optical motion capture analysis and its use with a multi-segment foot model has not been previously performed to our knowledge. With the four-segment model of Jenkyn and Anas [11], four of the possible six intersegmental motions were examined. The other two could not be measured with the fluoroscopic RSA system and the current testing protocol since the field of view was too small to image the ankle joint or the hallux. Of the four intersegmental joint motions examined, there were no significant differences found between optical motion capture and fluoroscopic RSA for motions of the hindfoot and forefoot. But the MLA height-to-length ratio was significantly different at midstance and toe off.

The intersegmental kinematics measured in this study with the multi-segment foot model agree with the results of Jenkyn and Anas [11]. Early in the stance phase, the hindfoot tended to pronate and internally rotate. It then tended to supinate and externally rotate at the approach of toe off. This accompanied the MLA height-to-length ratio that showed an initially depressing arch early in the stance phase and a rising arch later in the stance phase. The forefoot in this study tended to pronate early in the stance and then supinate as toe off approached. This is all consistent with a pronated and flexible foot early in the stance phase and a supinate and rigid foot configuration later in the stance phase.

A fluoroscopic RSA study by Arndt et al. [17] calculated kinematics within the foot slightly differently than the current study. Joint motions were reported between individual bones of the foot rather than between functional segments of the foot. The mean range of motion of the calcaneus with respect to the talus in the frontal plane was 8.9°. This joint motion is a good approximation of the supination/pronation movement of the hindfoot tested in our current study, which had a mean range of motion of 8.05° [17]. The other joint motions from the Arndt et al. [17] study had too dissimilar definitions to serve as reliable comparisons.

The MLA height-to-length ratio kinematics showed the smallest difference between optical motion capture and fluoroscopic RSA. The differences found were 0.00, 0.02, and 0.05, respectively, for heel strike, midstance, and toe off. Therefore, the measurement of the MLA during walking gait can be reliably performed using a multi-segment foot model and optical motion capture. In a clinical setting, the behaviour of the MLA is of diagnostic value for determining foot pathology. High-arched (pes cavus) individuals tend to have a more raised and rigid arch, which limits shock absorption in early stance [18]. Williams et al. [19] found that high-arched individuals with more mobile arches displayed smaller initial loading forces as well as lower forces at the second vertical ground reaction force peak during the loading phase [19]. Flat-footed (pes planus) individuals tend to have difficulty with force production later in the stance phase. Chang et al. [20] found that individuals with low arches had increased ground reaction forces peaks during two-foot drop landings when compared to normal feet [20]. Thus, quantifying the MLA height-to-length ratio could also be used to dynamically categorize the pathological foot type [18].

Hindfoot internal/external rotation showed the next smallest difference between optical motion capture and fluoroscopic RSA. Differences were found to be 1.33°, 0.45°, and 0.95° for heel strike, midstance, and toe off, respectively, with the greatest difference seen at heel strike. This may be due to increased muscle contraction around the ankle and subtalar joints causing the markers to move relative to the underlying bone. The hindfoot

marker cluster is placed adjacent to the peroneus longus and brevis tendon pathways. It is perhaps the tendon motion that partially influences the marker cluster positioning. It is interesting to note that hindfoot internal/external rotation is the least variable difference between test subjects [21].

Hindfoot supination/pronation motion had differences between optical motion capture and fluoroscopic RSA of 4.45° , 5.12° , and 6.70° for heel strike, midstance, and toe off, respectively. There was also a greater range of 15.80° measured with optical motion capture than for fluoroscopic RSA, 8.05° . This is consistent with the literature, which found that frontal plane markers and bone markers had poor agreement. Three studies found greater errors in skin-mounted markers relative to the underlying bone in the frontal area of the knee during running [22], in the ankle [17,23,24], and in the foot [23,24]. These studies addressed the same issue of validation as in the current study and found that while the range of motion was larger with optical techniques, the mean measurements were in relatively good agreement [17,22,23].

The greatest difference between optical motion capture and fluoroscopy was in the supination/pronation motion of the forefoot. The differences seen between motion capture and fluoroscopy were 7.68° , 1.81° , and 13.63° for heel strike, midstance, and toe off, respectively, with the greatest difference at toe off. The tibialis anterior muscle is primarily responsible for dorsi-flexing the foot at toe off. Its tendon inserts on the dorsal surface of the first cuneiform, close to the midfoot marker cluster. Therefore, contraction of the tibialis anterior may be influencing the position of this cluster [21]. The range for this joint was 18.27° as measured by optical motion capture versus 10.18° for fluoroscopic RSA.

One difficulty using a multi-segment foot model is that significantly more markers must be placed on the foot than when the foot is tracked as a single rigid segment. Five marker clusters are placed on the foot with the current model, with three on the medial side of the foot. With small feet, these clusters can be too close together for reliable tracking.

This study had limitations. The sample size was small due to the difficulty of collecting and analysing bi-planar fluoroscopic RSA data. Work is currently underway in our facility to increase this initial sample size. Future studies should examine the influence of pes cavus and pes planus foot types since the intersegmental motion within the foot is also very likely to be different with these foot pathologies, as the MLA behaviour has been shown to be. Validating the multi-segment foot model during walking and running in shoes should also be performed. Shoes may restrict the intersegmental motion of the foot segments and control the rise and fall of the MLA.

5. Conclusions

This study validates a multi-segment foot model that employs auto-reflective marker clusters and optical motion capture, benchmarked against bi-planar RSA fluoroscopy for accurate kinematic measurement. The comparison of hindfoot inversion/eversion and supination/pronation with respect to the midfoot, as well as forefoot supination/pronation with respect to the midfoot, revealed no significant differences between the two methods.

Clinically, the model's ability to measure the medial longitudinal arch (MLA) height-to-length ratio, which showed a significant difference only during the midstance and toe off phases of the stance phase, is noteworthy. The trend towards greater differences between motion capture and fluoroscopy during heel strike and toe off is attributed to increased muscular contraction for stabilization and push-off, causing more marker movement. Despite this, the lack of significant differences overall supports the multi-segment foot model's clinical utility, offering a viable alternative to fluoroscopy. This model reduces patient exposure to X-ray radiation and minimizes post-processing time, making it a practical tool for clinical settings.

Author Contributions: A.V. contributed to study design, data collection, and statistical analysis, interpretation of results. K.B. contributed to data processing and method development. T.J. contributed to conceptualization and design of the study, interpretation of results and drafting of the manuscript. All authors have read and agreed to the published version of the manuscript.

Funding: This work was supported by the Natural Science and Engineering Research Council (NSERC) of Canada RGPIN-2016-04439 and by a Transdisciplinary Training Award from the University of Western Ontario’s Bone and Joint Institute.

Institutional Review Board Statement: The study was conducted in accordance with the Declaration of Helsinki, and approved by the Institutional Review Board (or Ethics Committee) of the University of Western Ontario (protocol 119712, approved 10 November 2017).

Informed Consent Statement: Informed consent was obtained from all subjects involved in the study.

Data Availability Statement: The data presented in this study are available on request from the corresponding author.

Conflicts of Interest: The authors declare no conflicts of interest.

References

- Schallig, W.; van den Noort, J.C.; Piening, M.; Streekstra, G.J.; Maas, M.; van der Krogt, M.M.; Harlaar, J. The Amsterdam Foot Model: A clinically informed multi-segment foot model developed to minimize measurement errors in foot kinematics. *J. Foot Ankle Res.* **2022**, *15*, 46–61. [\[CrossRef\]](#) [\[PubMed\]](#)
- Wager, J.C.; Challis, J.H. Mechanics of the foot and ankle joints during running using a multi-segment foot model compared with a single-segment model. *PLoS ONE* **2024**, *19*, e0294691. [\[CrossRef\]](#) [\[PubMed\]](#)
- Matias, A.B.; Caravaggi, P.; Leardini, A.; Taddei, U.T.; Ortolani, M.; Sacco, I. Repeatability of skin-marker based kinematics measures from a multi-segment foot model in walking and running. *J. Biomech.* **2020**, *110*, 109983. [\[CrossRef\]](#)
- Leardini, A.; Caravaggi, P.; Theologis, T.; Stebbins, J. Review: Multi-segment foot models and their use in clinical populations. *Gait Posture* **2019**, *69*, 50–59. [\[CrossRef\]](#)
- Kuska, E.C.; Barrios, J.A.; Kinney, A.L. Multi-segment foot model reveals distal joint kinematic differences between habitual heel-toe walking and non-habitual toe walking. *J. Biomech.* **2020**, *110*, 109960. [\[CrossRef\]](#)
- Kim, E.J.; Shin, H.S.; Lee, J.H.; Kyung, M.G.; Yoo, H.J.; Yoo, W.J.; Lee, D.Y. Repeatability of a multi-segment foot model with a 15-marker set in normal children. *Clin. Orthop. Surg.* **2018**, *10*, 484–490. [\[CrossRef\]](#)
- Fritz, J.M.; Canseco, K.; Konop, K.A.; Kruger, K.M.; Tarima, S.; Long, J.T.; Law, B.C.; Kraus, J.C.; King, D.M.; Harris, G.F. Multi-segment foot kinematics during gait following ankle arthroplasty. *J. Orthop. Res.* **2021**, *40*, 685–694. [\[CrossRef\]](#)
- Klein, T.; Chapman, G.J.; Lastovicka, O.; Janura, M.; Richards, J. Do different multi-segment foot models detect the same changes in kinematics when wearing foot orthoses? *J. Foot Ankle Res.* **2022**, *15*, 68–77. [\[CrossRef\]](#)
- Jang, W.Y.; Lee, D.Y.; Jung, H.W.; Lee, D.J.; Yoo, W.J.; Choi, I.H. Inter-segment foot motion in girls using a three-dimensional multi-segment foot model. *Gait Posture* **2018**, *63*, 184–188. [\[CrossRef\]](#)
- Matsumoto, Y.; Ogihara, N.; Hanawa, H.; Kokubun, T.; Kanemura, N. Novel multi-segment foot model incorporating plantar aponeurosis for detailed kinematic and kinetic analyses of the foot with application to gait studies. *Front. Bioeng. Biotechnol.* **2022**, *10*, 894731. [\[CrossRef\]](#)
- Jenkyn, T.R.; Anas, K.; Nichol, A. Foot segment kinematics during normal walking using a multisegment model of the foot and ankle complex. *J. Biomech. Eng.* **2009**, *131*, 034504. [\[CrossRef\]](#) [\[PubMed\]](#)
- Hulshof, C.M.; Schallig, W.; van den Noort, J.C.; Streekstra, G.J.; Kleipool, R.P.; Dobbe, J.G.; Maas, M.; Harlaar, J.; van der Krogt, M.M. Skin marker-based versus bone morphology-based coordinate systems of the hindfoot and forefoot. *J. Biomech.* **2024**, *166*, 112001. [\[CrossRef\]](#) [\[PubMed\]](#)
- Roach, K.E.; Foreman, K.B.; MacWilliams, B.A.; Karpos, K.; Nichols, J.; Anderson, A.E. The modified Shriners Hospitals for Children Greenville (mSHCG) multi-segment foot model provides clinically acceptable measurements of ankle and midfoot angles: A dual fluoroscopy study. *Gait Posture* **2022**, *85*, 258–265. [\[CrossRef\]](#) [\[PubMed\]](#)
- Maharaj, J.N.; Rainbow, M.J.; Cresswell, A.G.; Kessler, S.; Konow, N.; Gehring, D.; Lichtwark, G.A. Modelling the complexity of the foot and ankle during human locomotion: The development and validation of a multi-segment foot model using biplanar videoradiography. *Comput. Methods Biomech. Biomed. Eng.* **2022**, *25*, 554–565. [\[CrossRef\]](#)
- Kedgley, A.E.; Birmingham, T.; Jenkyn, T.R. Comparative accuracy of radiostereometric and optical tracking systems. *J. Biomech.* **2009**, *42*, 1350–1354. [\[CrossRef\]](#)
- Valevicius, A. Validation of the Multi-Segment Foot Model with Bi-Planar Fluoroscopy (ETD No. 2633). Master’s Thesis, University of Western Ontario, London, ON, Canada, 2014.
- Arndt, A.; Wolf, P.; Liu, A.; Nester, C.; Stacoff, A.; Jones, R.; Lundgren, P.; Lundberg, A. Intrinsic foot kinematics measured in vivo during the stance phase of slow running. *J. Biomech.* **2007**, *40*, 2672–2678. [\[CrossRef\]](#)
- Stone, A.; Stender, C.J.; Whittaker, E.C.; Hahn, M.E.; Rohr, E.; Cowley, M.S.; Sangeorzan, B.J.; Ledoux, W.R. Ability of a multi-segment foot model to measure kinematics differences in cavus, neutrally aligned, asymptomatic planus, and symptomatic planus foot types. *Gait Posture* **2024**, *113*, 452–461. [\[CrossRef\]](#)
- Williams, D.S.B.; Tierney, R.N.; Butler, R.J. Increased medial longitudinal arch mobility, lower extremity kinematics, and ground reaction forces in high-arched runners. *J. Athl. Train.* **2014**, *49*, 290–296. [\[CrossRef\]](#)

20. Chang, J.S.; Kwon, Y.H.; Kim, C.S.; Ahn, S.-H.; Park, S.H. Differences of ground reaction forces and kinematics of lower extremity according to landing height between flat and normal feet. *J. Back Musculoskelet. Rehabil.* **2012**, *25*, 21–26. [[CrossRef](#)]
21. Shultz, R.; Kedgley, A.; Jenkyn, T. Quantifying skin motion artifact error of the hindfoot and forefoot marker clusters with the optical tracking of a multi-segment foot model using single-plane fluoroscopy. *Gait Posture* **2011**, *34*, 44–48. [[CrossRef](#)]
22. Gale, T.; Anderst, W. Knee kinematics of healthy adults measured using biplane radiography. *J. Biomech. Eng.* **2020**, *142*, 101004. [[CrossRef](#)] [[PubMed](#)]
23. Schallig, W.; Streekstra, G.J.; Hulshof, C.M.; Kleipool, R.P.; Dobbe, J.G.; Maas, M.; Harlaar, J.; van der Krogt, M.M.; van den Noort, J.C. The influence of soft tissue artifacts on multi-segment foot kinematics. *J. Biomech.* **2021**, *120*, 110359. [[CrossRef](#)] [[PubMed](#)]
24. Nester, C.; Jones, R.; Liu, A.; Howard, D.; Lundberg, A.; Arndt, A.; Lundgren, P.; Stacoff, A.; Wolf, P. Foot kinematics during walking measured using bone and surface mounted markers. *J. Biomech.* **2007**, *40*, 3412–3423. [[CrossRef](#)] [[PubMed](#)]

Disclaimer/Publisher’s Note: The statements, opinions and data contained in all publications are solely those of the individual author(s) and contributor(s) and not of MDPI and/or the editor(s). MDPI and/or the editor(s) disclaim responsibility for any injury to people or property resulting from any ideas, methods, instructions or products referred to in the content.